

Quantum dissipative dynamics of the magnetic resonance force microscope in the single-spin detection limit

Hanno Gassmann*

Department of Physics and Astronomy, University of Basel, Klingelbergstrasse 82, 4056 Basel, Switzerland

Mahn-Soo Choi[†]

Department of Physics, Korea University, Seoul 136-701, Korea

Hangmo Yi

Korea Institute for Advanced Study, 207-43 Cheongryang 2-dong, Seoul 130-722, Korea

C. Bruder

Department of Physics and Astronomy, University of Basel, Klingelbergstrasse 82, 4056 Basel, Switzerland

(Received 19 September 2003; published 22 March 2004)

We study a model of a magnetic resonance force microscope (MRFM) based on the cyclic adiabatic inversion technique as a high-resolution tool to detect single electron spins. We investigate the quantum dynamics of spin and cantilever in the presence of coupling to an environment. To obtain the reduced dynamics of the combined system of spin and cantilever, we use the Feynman-Vernon influence functional and get results valid at any temperature as well as at arbitrary system-bath coupling strength. We propose that the MRFM can be used as a quantum measurement device, i.e., not only to detect the modulus of the spin but also its direction.

DOI: 10.1103/PhysRevB.69.115419

PACS number(s): 03.65.Yz, 07.79.Pk, 07.10.Cm

I. INTRODUCTION

Magnetic resonance imaging technologies (MRI, NMR, ESR) are widely used to characterize physical, chemical, and biological samples. What makes them powerful is that they are nondestructive and capable to probe the three-dimensional structure of the sample.¹ Recently, looking at structures at the molecular or atomic level has become important in a number of scientific disciplines. Magnetic resonance force microscopes (MRFMs) have been developed to bring magnetic resonance imaging technologies to such an ultimate resolution. The MRFM combines conventional magnetic resonance technology with probe microscope technology, e.g., atomic force microscopy, to image individual molecules or atoms.² In a MRFM, a magnetic particle mounted on a cantilever interacts with nuclear or electron spins in the sample via the very weak magnetic dipole force. When modulated at resonance with the cantilever oscillation frequency, even a weak magnetic force induces sufficiently large vibrations of the cantilever. By probing the resulting vibrational motion of the cantilever, it is in principle possible to detect spins with molecular or atomic resolution. The cyclic adiabatic inversion (CAI) technique has been proposed² as a promising method to modulate the magnetic force.

The future of the MRFM depends crucially on the development of proper mechanical microresonators, e.g., cantilevers.³ Remarkable progress has been made in this direction, and the detection of atto-newton or subatto-newton scale forces has been achieved already.^{4,5} Recently, a nanomechanical flexural resonator at microwave frequencies has also been realized.⁶ The development of the proper technology to detect nanometer-scale mechanical motion is also important. Optical interferometry or electrical parametric transducers are the most common examples.^{4,5,7} In recent work, a single-electron transistor capacitively coupled to a nanome-

chanical resonator has been used to detect the vibrational motion of the resonator even in the quantum regime.⁸

The progress in MRFM and related technologies has also attracted theoretical interest, especially the question of single-spin detection using the MRFM. Mozyrsky *et al.*⁹ studied the relaxation of a spin, treating the cantilever as a classical noise source. Berman and co-workers^{10,11} studied a CAI-based MRFM and treated both the spin and the cantilever as quantum systems that are subject to environmental effects. They addressed two interesting and important issues: which component is measured in an MRFM single-spin measurement and whether the two spin states (up and down) lead to distinctively different cantilever motions. They solved numerically the time-dependent Schrödinger equation for the spin-plus-cantilever system in the absence of coupling to the environment. In the presence of an environment, they constructed a generalized master equation in the high-temperature limit, and solved it numerically. We note that their master equation is based on the Markov approximation, and is not in Lindblad form^{12,13} (the normalization and the positivity of the density matrix are not guaranteed).

In this paper, we study the measurement of single spins with the MRFM based on the CAI technique. The starting point of our work is closely related to Refs. 10 and 11. In the absence of the coupling to the environment, we solve the time-dependent Schrödinger equation exactly and confirm the numerical results by Berman and co-workers.^{10,11} We use an open quantum system approach,^{14,15} i.e., we take the influence of the environment into account by coupling a harmonic oscillator bath to the cantilever. To calculate the dynamics of the spin during the measurement process, we take an effective-bath approach, and obtain the exact solution for the reduced density matrix of the spin. To find the cantilever dynamics, we solve the Feynman-Vernon influence functional^{16,17} in order to obtain the reduced density matrix

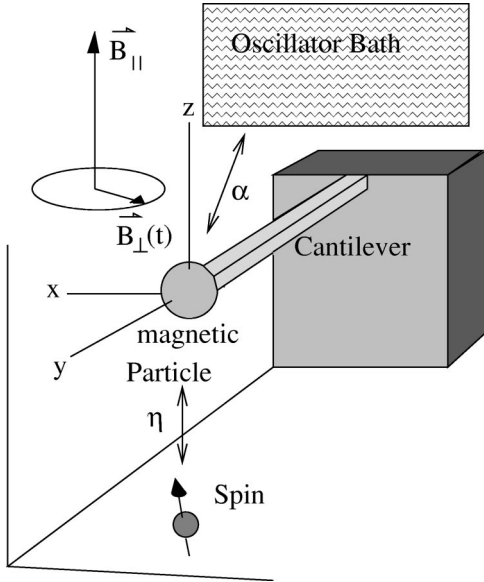


FIG. 1. MRFM measurement device. A cantilever carrying a magnetic particle is subject to a static magnetic field \mathbf{B}_{\parallel} in the z -direction, and a time-dependent field $\mathbf{B}_{\perp}(t)$ rotating with frequency ω_{rf} in the x - y plane. The cantilever is coupled to a sample spin by a magnetic force η .

of the spin plus cantilever system. Both methods are valid at any temperature as well as for an arbitrary coupling strength (within the CAI scheme). This analytical approach allows us to interpret the results in a transparent way and to investigate the issue whether the MRFM can be used as a quantum measurement device to probe the spin state.

The paper is organized as follows: In Sec. II we first introduce the model and discuss our adiabatic Born-Oppenheimer approximation scheme in connection with the CAI technique. In Sec. III we present the exact solution of the time-dependent Schrödinger equation for the spin-plus-cantilever system without coupling to the environment, the results of which will be compared with those in the dissipative case in the later sections. In Sec. IV, we investigate the quantum dissipative dynamics of the spin alone using an effective-bath approach. The dynamics of the cantilever is investigated in Sec. V. The physical implications of the solution are analyzed in detail and the possibility to use the MRFM as a quantum measurement device is discussed in Sec. VI. Finally, in Sec. VII we draw our conclusions.

II. MODEL

We consider a MRFM setup based on the cyclic adiabatic inversion technique (see Fig. 1). It consists of a ferromagnetic particle mounted on the tip of a cantilever, a strong static magnetic field \mathbf{B}_{\parallel} in the z direction, and an rf field $\mathbf{B}_{\perp}(t)$ rotating with frequency ω_{rf} in the x - y plane modulated by $\phi(t)$:

$$\mathbf{B}_{\perp}(t) = B_{\perp} \begin{bmatrix} \cos[\omega_{\text{rf}}t - \phi(t)] \\ -\sin[\omega_{\text{rf}}t - \phi(t)] \end{bmatrix}. \quad (2.1)$$

As in usual NMR setups, one puts $\omega_{\text{rf}} = \epsilon_z \equiv g\mu_B B_{\parallel}$, where g is the g factor of the spin and μ_B is the Bohr magneton. For later use, we also define $\epsilon_{\perp} \equiv g\mu_B B_{\perp}$. The “sample” consists of a spin interacting with the ferromagnetic particle via the magnetic force η and with the static and rf fields. The Hamiltonian of the spin and the cantilever is given by

$$\mathcal{H}(t) = -\frac{\epsilon_z}{2}\hat{\sigma}_z - \frac{\epsilon_{\perp}}{2}[\hat{\sigma}_+ e^{i\epsilon_z t - i\phi(t)} + \text{H.c.}] - \eta\hat{\sigma}_z \hat{z} + \frac{\hat{p}_z^2}{2} + \frac{\hat{z}^2}{2}, \quad (2.2)$$

where the $\hat{\sigma}$'s are Pauli matrices, $\hat{\sigma}_{\pm} = (\hat{\sigma}_x \pm i\hat{\sigma}_y)/2$, and \hat{z} (\hat{p}_z) is the position (momentum) operator of the cantilever. In Eq. (2.2) and hereafter we use a unit system such that $\hbar = k_B = \omega_0 = \ell_0 = 1$, where ω_0 is the natural frequency of the cantilever and $\ell_0 \equiv \sqrt{\hbar/m\omega_0}$ is the harmonic-oscillator length. It is convenient to move to a frame rotating with the rf field by making a transformation¹⁸

$$\mathcal{H} \rightarrow \mathcal{A}^{\dagger} \mathcal{H} \mathcal{A} - i\mathcal{A}^{\dagger} \dot{\mathcal{A}} \quad (2.3)$$

with $\mathcal{A} = \exp\{(i/2)[\epsilon_z t - \phi(t)]\hat{\sigma}_z\}$. The resulting Hamiltonian reads^{10,11}

$$\mathcal{H}(t) = -\frac{1}{2}\dot{\phi}(t)\hat{\sigma}_z - \frac{1}{2}\epsilon_{\perp}\hat{\sigma}_x - \eta\hat{\sigma}_z \hat{z} + \frac{\hat{p}_z^2}{2} + \frac{\hat{z}^2}{2}. \quad (2.4)$$

The idea of the CAI-based MRFM is as follows: The phase modulation $\phi(t)$ of the rf field is assumed to be harmonic and causes adiabatic inversions of the spin, which in turn exert an oscillating force on the cantilever. At resonance, i.e., if the frequency of the modulation is equal to the natural frequency of the cantilever (which is 1 in our units),

$$\dot{\phi}(t) = \phi_0 \sin(t - \varphi), \quad (2.5)$$

the vibration amplitude of the cantilever can be large even for a very small magnetic force η .

Equation (2.4) describes a spin which couples to a harmonic oscillator and is itself subject to a time-dependent effective magnetic field $g\mu_B \mathbf{B}_{\text{eff}}(t) \equiv \epsilon_{\perp} \mathbf{e}_x + \dot{\phi}(t) \mathbf{e}_z$, where \mathbf{e}_x and \mathbf{e}_z are unit vectors in the rotating system. The Hamiltonian in Eq. (2.4) is not exactly solvable. Here we make a plausible approximation based on the following observations. For typical experimental parameters,^{10,11} \mathbf{B}_{eff} varies slowly compared with the Rabi oscillation frequency: $|\dot{\mathbf{B}}_{\text{eff}}(t)|/|\mathbf{B}_{\text{eff}}(t)| \ll \epsilon(t) \equiv \sqrt{\epsilon_{\perp}^2 + \dot{\phi}^2(t)}$. According to the adiabatic theorem,^{18,19} the spin part of the solution should be determined by the adiabatic evolution; i.e., the spin “follows adiabatically” the effective field $\mathbf{B}_{\text{eff}}(t)$. It is therefore convenient to choose the basis states $|\chi_+(t)\rangle$ and $|\chi_-(t)\rangle$ quantized along the axis parallel to $\mathbf{B}_{\text{eff}}(t)$ (notice that there is no Berry phase because the solid angle enclosed by $\mathbf{B}_{\text{eff}}(t)$ is zero). In this basis, the Hamiltonian in Eq. (2.4) is recast to

$$\mathcal{H}(t) = -\frac{1}{2}\epsilon(t)\hat{\tau}_z - \eta \frac{\dot{\phi}(t)}{\epsilon(t)} \hat{\tau}_z \hat{z} + \eta \frac{\epsilon_{\perp}}{\epsilon(t)} \hat{\tau}_x \hat{z} + \frac{\hat{p}_z^2}{2} + \frac{\hat{z}^2}{2}, \quad (2.6)$$

where $\hat{\tau}_x$ and $\hat{\tau}_z$ are the Pauli matrices with respect to the frame rotating adiabatically with $\mathbf{B}_{\text{eff}}(t)$. We have suppressed the time arguments to the Pauli matrices $\hat{\tau}_z(t) \equiv |\chi_+(t)\rangle\langle\chi_+(t)| - |\chi_-(t)\rangle\langle\chi_-(t)|$ and $\hat{\tau}_x(t) \equiv |\chi_+(t)\rangle\langle\chi_-(t)| + |\chi_-(t)\rangle\langle\chi_+(t)|$ in Eq. (2.6). This is because within the adiabatic approximation, the dynamics of the spin part of the wave function is completely governed by the basis states $|\chi_{\pm}(t)\rangle$ and the dynamic phases, i.e., $|\chi(t)\rangle = c_+ e^{-i\int_0^t dt' \epsilon_+(t')} |\chi_+(t)\rangle + c_- e^{-i\int_0^t dt' \epsilon_-(t')} |\chi_-(t)\rangle$. We further note that the spin dynamics is much faster than the cantilever motion, $\epsilon(t) \gg \epsilon_{\perp} \gg 1$. The situation is reminiscent of the Born-Oppenheimer approximation,²⁰ where the nuclei interact with the average charge density of the electrons which move much faster. In our system the nuclei correspond to the harmonic oscillator which is interacting with the averaged motion of the spin. Therefore, one can drop the third term in Eq. (2.6). (The deviation of the spin due to this term is also negligibly small since $\eta|\langle\hat{z}(t)\rangle| \ll \epsilon(t)$; see below.) Using this approximation we finally get the following Hamiltonian, which is the basis of the further considerations in the paper:

$$\mathcal{H}(t) = -\frac{1}{2}\epsilon(t)\hat{\tau}_z - \eta f(t)\hat{\tau}_z\hat{z} + \frac{\hat{p}_z^2}{2} + \frac{\hat{z}^2}{2}, \quad (2.7)$$

where $f(t) \equiv \dot{\phi}(t)/\epsilon(t)$. This form is justified in a more rigorous way in Appendix A, also taking into account the influence of the environment (see below). Its validity was also confirmed by the numerical simulations in Ref. 11.

So far we have described a model for an idealized system of spin and cantilever. In reality they are coupled to various environments, which lead to decoherence as well as damping. In particular, the cantilever is inevitably under the influence of phonons or other vibrational modes which are close in frequency to the single mode in question. The (direct) environmental effects for the spin, e.g., hyperfine interaction, spin-lattice relaxation, etc., are relatively small. Therefore, for simplicity, we assume a simple Ohmic bath of oscillators^{15,21-23} directly coupled to the cantilever but not to the spin. Then the total Hamiltonian for the spin and the cantilever plus the oscillator bath is given by

$$\mathcal{H}_{\text{total}}(t) = \mathcal{H}(t) + \sum_{k=1}^{\infty} \left[\frac{\hat{p}_k^2}{2m_k} + \frac{m_k \omega_k^2}{2} \left(\hat{x}_k - \frac{c_k}{m_k \omega_k^2} \hat{z} \right)^2 \right]. \quad (2.8)$$

All the relevant features of the Ohmic bath are characterized by the spectral density

$$J(\omega) = \frac{\pi}{2} \sum_k \frac{c_k^2}{m_k \omega_k} \delta(\omega - \omega_k) = \alpha \omega \Theta(1 - \omega/\omega_C), \quad (2.9)$$

where α is a dimensionless parameter characterizing the coupling between the system and the environment and ω_C is the cutoff frequency. The spin dynamics and the probability distribution of the cantilever will not depend on the cutoff.

We describe the system of spin plus cantilever in terms of the reduced density matrix $\hat{\rho}(t) \equiv \text{tr}_B \hat{\rho}_{\text{tot}}(t)$ by tracing out the bath. In the realistic typical experimental situation, the cantilever always remains in contact with the environment. Thus, the cantilever and bath are not in a product state at the beginning of the experiment. For the calculation with the influence functional, we can take this fact into account, assuming that the cantilever and the bath were in a factorized state at a time $t=t_0$. In the limit $t_0 \rightarrow -\infty$ we get then the realistic initial state for the cantilever at the time $t=0$. If we would start with a factorized state between cantilever and bath, the solution would be very sensitive to the initial condition of the cantilever; see Sec. IV.

Furthermore, it is assumed that the interaction between the spin and the cantilever is turned on at $t=0$, i.e., $f(t)=0$ for $t<0$. The measurement happens at times $t>0$. The initial state $\hat{\rho}(0)$ of the density matrix is a product state,

$$\hat{\rho}(0) = \hat{\rho}^{(S)}(0) \hat{\rho}^{(C)}(0), \quad (2.10)$$

where $\hat{\rho}^{(S)}$ is the density matrix for the spin only and $\hat{\rho}^{(C)}$ describes the cantilever in thermal equilibrium with the bath. From the CAI scheme and from the associated adiabatic approximation discussed above it then follows that the density matrix at times $t>0$ has the form

$$\langle s, z | \hat{\rho}(t) | s', z' \rangle = \rho_{ss'}^{(S)}(0) \rho_{ss'}^{(C)}(z, z', t). \quad (2.11)$$

Thus, the dynamics of the density matrix $\hat{\rho}(t)$ is completely determined by the spin-dependent cantilever part $\rho_{ss'}^{(C)}(z, z', t)$.

Here the spin-dependent cantilever part should not be confused with the density matrix for the cantilever only, which is given by

$$\begin{aligned} \rho^{(C)}(z, z', t) &= \sum_{s=\pm} \langle s, z | \hat{\rho}(t) | s, z' \rangle \\ &= \rho_{++}^{(S)}(0) \rho_{++}^{(C)}(z, z', t) \\ &\quad + \rho_{--}^{(S)}(0) \rho_{--}^{(C)}(z, z', t). \end{aligned} \quad (2.12)$$

Analogously, the density matrix for the spin only at time $t>0$ is given by

$$\rho_{ss'}^{(S)}(t) = \rho_{ss'}^{(S)}(0) \int_{-\infty}^{\infty} dz \rho_{ss'}^{(C)}(z, z, t). \quad (2.13)$$

There are several ways to prepare the spin in a particular state,¹⁵ and we will assume a general state $\rho_{ss'}^{(S)}(0)$.

III. COHERENT SOLUTION WITHOUT BATH

Before we investigate the full Hamiltonian in Eq. (2.8), it will be instructive to first consider the problem without bath [Eq. (2.7)]. The time-dependent Hamiltonian in Eq. (2.7) can be solved exactly for arbitrary functions $\epsilon(t)$ and $f(t)$ of t (of course, the variation of $\epsilon(t)$ and $f(t)$ in time should be sufficiently slow so that the Hamiltonian Eq. (2.7) is meaningful).

One can show that the time-evolution operator $\mathcal{U}(t_2, t_1) \equiv \hat{T} \exp[-i \int_{t_1}^{t_2} dt' \mathcal{H}(t')] \hat{T}$ (\hat{T} is the time-ordering operator) is given by

$$\mathcal{U}(t_2, t_1) = \exp \left[ic(t_1, t_2) + \frac{i}{2} \int_{t_1}^{t_2} dt' \epsilon(t') \hat{\tau}_z \right] \times \mathcal{D}(\hat{\tau}_z \xi(t_2)) \mathcal{U}_0(t_2 - t_1) \mathcal{D}^\dagger(\hat{\tau}_z \xi(t_1)), \quad (3.1)$$

where

$$\xi(t) \equiv i \eta \frac{1}{\sqrt{2}} \int_0^t dt' e^{-i(t-t')} f(t'), \quad (3.2)$$

$$\mathcal{U}_0(t) \equiv \exp(-it \hat{a}^\dagger \hat{a}), \quad (3.3)$$

$\hat{a} = (\hat{z} + i \hat{p}_z) / \sqrt{2}$, and $\mathcal{D}(\xi)$ is a displacement operator²⁴ defined for a complex number ξ by

$$\mathcal{D}(\xi) = \exp(\xi \hat{a}^\dagger - \xi^* \hat{a}). \quad (3.4)$$

The coefficient $c(t_1, t_2)$ in Eq. (3.1) is a real function of t_1 and t_2 (one does not need an explicit expression of it because it drops out of the following calculations).

To illustrate the dynamics created by the time-evolution operator in Eq. (3.1), let us discuss an example. Suppose that we start at time $t=0$ with the cantilever in a coherent state,

$$\psi(z, 0) = \frac{1}{\sqrt{4\pi}} \exp \left[-\frac{1}{2} z^2 + \sqrt{2} \xi_0 z - (\text{Re } \xi_0)^2 \right], \quad (3.5)$$

and with the spin in a linear superposition (with amplitudes c_+ and c_-)

$$|\chi(0)\rangle = c_+ |\chi_+(0)\rangle + c_- |\chi_-(0)\rangle. \quad (3.6)$$

The total wave function at $t=0$ is given by

$$|\Psi(z, 0)\rangle = \psi(z, 0) |\chi(0)\rangle, \quad (3.7)$$

and, at a later time $t > 0$, by

$$|\Psi(z, t)\rangle = c_+ \psi_+(z, t) |\chi_+(t)\rangle + c_- \psi_-(z, t) |\chi_-(t)\rangle. \quad (3.8)$$

The cantilever wave function in Eq. (3.8) for each spin component is given by

$$\psi_\pm(z, t) = \frac{1}{\sqrt{4\pi}} \exp \left[ic(t, 0) \pm i \int_0^t dt' \epsilon(t') \right] \times \exp \left\{ -\frac{1}{2} z^2 + \sqrt{2} \xi'_\pm(t) z - [\text{Re } \xi'_\pm(t)]^2 \right\}, \quad (3.9)$$

where

$$\xi'_\pm(t) = \pm \xi(t) + \xi_0 e^{-it}. \quad (3.10)$$

Therefore, the average position of the cantilever is $\langle \hat{z}(t) \rangle_\pm = \sqrt{2} \text{Re } \xi'_\pm(t)$ for spin $s = \pm$, respectively, whereas the average momentum is given by $\langle \hat{p}_z(t) \rangle_\pm = \sqrt{2} \text{Im } \xi'_\pm(t)$. Here it is interesting to note (in comparison with the results be-

low) that exactly at resonance [see Eq. (2.5)], $|\xi(t)|$ in Eq. (3.2) [and hence $|\xi'_\pm(t)|$ in Eq. (3.10)] contains a term which linearly increases with time t . In other words, the oscillation amplitude of the cantilever gets indefinitely larger and larger as time passes. This is not surprising since we are driving an *ideal* oscillator at the resonance frequency, and in fact this is what allows the MRFM to detect ultrasmall forces. In reality, the cantilever is subject to various environmental effects and the oscillation amplitude is bounded from above (i.e., the Q factor is finite). This is the case that we will study below.

IV. DYNAMICS OF THE SPIN

Now we take the influence of the bath into account. In this section, we first analyze the dynamics of the spin. As described above [see the discussion above Eq. (2.8)], there are several environmental effects for the spin. In this calculation, we assume that such effects directly cause the spin to be small compared to the interaction with the measuring device, i.e., the cantilever coupled to the oscillator bath. Thus, the decoherence time of the spin in the absence of the cantilever is assumed much longer than the time we need for the measurement. These different time scales are necessary to provide cyclic inversions of the spin.

A similar situation appears in the well-known Stern-Gerlach experiment, where the environment first collapses the trajectory of the particle which then causes the collapse of the spin. As in our calculation, other decoherence mechanisms, which act directly on the spin, are neglected.

When we are interested in the dynamics of the spin alone (the dynamics of the cantilever will be discussed in the following section), we can regard the cantilever as a part of the environment. In fact, Garg *et al.*²⁵ (also see Refs. 26–28) showed that the problem is equivalent to a spin coupled linearly to an oscillator bath:

$$\mathcal{H}_{\text{tot}}(t) = -\frac{1}{2} \epsilon(t) \hat{\tau}_z - \eta f(t) \hat{\tau}_z \sum_k g_k (\hat{b}_k^\dagger + \hat{b}_k) + \sum_k \omega_k \hat{b}_k^\dagger \hat{b}_k. \quad (4.1)$$

The distribution of the oscillator frequencies ω_k and the coupling constant g_k are now characterized by a non-Ohmic spectral density

$$J_{\text{eff}}(\omega) \equiv \sum_k g_k^2 \delta(\omega - \omega_k) = \frac{1}{\pi} \frac{\alpha \omega}{(\omega^2 - 1)^2 + (\alpha \omega)^2}. \quad (4.2)$$

To investigate the spin dynamics, we write the reduced density matrix of the spin

$$\hat{\rho}^{(S)}(t) = \text{tr}_B \mathcal{U}_{\text{tot}}(t) \hat{\rho}_{\text{tot}}(0) \mathcal{U}_{\text{tot}}^\dagger(t) \quad (4.3)$$

in terms of the time-evolution operator $\mathcal{U}_{\text{tot}}(t)$ associated with $\mathcal{H}_{\text{tot}}(t)$ in Eq. (4.1). In analogy to Eq. (3.1), the time-evolution operator is given by

$$\mathcal{U}_{\text{tot}}(t) = \exp \left[\frac{i}{2} \int_0^t dt' \epsilon(t') \hat{\tau}_z \right] \prod_k \mathcal{D}(\hat{\tau}_z \xi_k(t)) e^{-i \omega_k t \hat{b}_k^\dagger \hat{b}_k}, \quad (4.4)$$

where

$$\xi_k(t) = i\eta g_k \int_0^t dt' e^{-i(t-t')\omega_k} f(t'), \quad (4.5)$$

and \mathcal{D} is now the displacement operator for the k th mode of the bath, i.e., \hat{a} should be replaced by \hat{b}_k in Eq. (3.4).

For the initial state $\hat{\rho}_{\text{tot}}(0)$, we assume [see Eqs. (2.10)]

$$\hat{\rho}_{\text{tot}}(0) = \hat{\rho}^{(S)}(0) \prod_k \frac{e^{-\beta\omega_k \hat{b}_k^\dagger \hat{b}_k}}{Z_k}. \quad (4.6)$$

Then the density matrix for the spin is given by

$$\begin{aligned} \rho_{ss'}^{(S)}(t) &= \rho_{ss'}^{(S)}(0) \exp\left[i \frac{(s-s')}{2} \int_0^t dt' \epsilon(t') \right] \\ &\times \prod_k \langle \mathcal{D}^\dagger(s' \xi_k(t)) \mathcal{D}(s \xi_k(t)) \rangle_k, \end{aligned} \quad (4.7)$$

where $\langle \dots \rangle_k$ is the average with respect to the k th oscillator in the bath.

Equation (4.7) shows that the diagonal elements of the density matrix ($s=s'$) are constant in time

$$\rho_{ss}^{(S)}(t) = \rho_{ss}^{(S)}(0). \quad (4.8)$$

In other words, there is no spin relaxation and the spin dynamics is pure dephasing because there are no transverse fields. This is consistent with the adiabatic approximation we made at the beginning.

On the other hand, the off-diagonal elements ($s \neq s'$) are expected to vanish rapidly with time. This can be seen from [see Eq. (4.7)]

$$\rho_{+-}^{(S)}(t) = \rho_{+-}^{(S)}(0) \exp\left[-\Gamma(t) + i \int_0^t dt' \epsilon(t') \right], \quad (4.9)$$

where

$$\Gamma(t) \equiv 2 \sum_k |\xi_k(t)|^2 \coth\left(\frac{\omega_k}{2T}\right), \quad (4.10)$$

or in terms of the spectral density function

$$\Gamma(t) = 2\eta^2 \int_0^\infty d\omega J_{\text{eff}}(\omega) \coth\left(\frac{\omega}{2T}\right) \left| \int_0^t dt' e^{i\omega t'} f(t') \right|^2. \quad (4.11)$$

Figure 2 shows $|\rho_{+-}^{(S)}(t)|$ evaluated using Eqs. (4.9) and (4.11). To compare our results with those of Berman and co-workers^{10,11} who assumed an initial product state of cantilever and bath, the inset of Fig. 2 shows $|\rho_{+-}^{(S)}(t)|$ for a Gaussian initial state of the cantilever. (To obtain these results we evaluate the path-integral formulas in Appendix B with $t_0=0$ instead of taking the limit $t_0 \rightarrow -\infty$.) If we compare the main part of Fig. 2 with the inset the strong dependence on the initial conditions is evident. The slower decay and more pronounced oscillations shown in the inset are a consequence of the oscillatory relaxation of the cantilever to its thermal equilibrium state if one starts with an initial product state of cantilever and bath. On increasing the coupling α , the oscillatory behavior becomes less visible since the cantilever relaxes immediately to its thermal state.

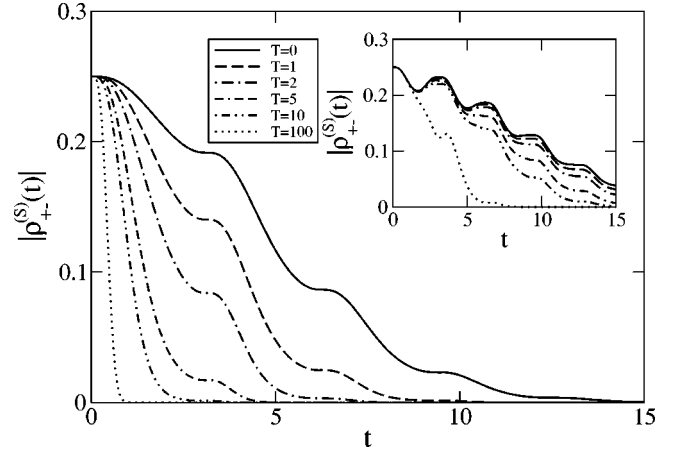


FIG. 2. Main plot: $|\rho_{+-}^{(S)}(t)|$ for different temperatures $T = 0, 1, 2, 5, 10,$ and 100 , for $\phi_0 = 1000$, $\epsilon_\perp = 400$, $\eta = 0.3$, $\alpha = 0.006$, and $\omega_c = 1000$. The initial condition for cantilever and bath is the thermal equilibrium state. Inset: same quantity for an initial product state of cantilever and bath. Initially, the cantilever wave function is a Gaussian with width $\sigma = \sqrt{2}$. In both cases, $\rho_{ss'}^{(S)}(0) = 1/2$ for $s, s' = \pm$.

V. DYNAMICS OF THE CANTILEVER

In Sec. III, we described the driven dynamics of the otherwise isolated system of spin and cantilever determined by the Hamiltonian Eq. (2.7). In this section, we now take into account the influence of the environment starting from the Hamiltonian Eq. (2.8). The reduced dynamics is obtained analytically with the Feynman-Vernon influence functional^{16,17} for arbitrary coupling strength α to the bath and for arbitrary temperature T . The advantage of this method as compared to Ref. 11 is that no master equation is used and that there is no restriction on the number of basis functions used to numerically integrate the problem.

The reduced dynamics of the cantilever obtained with the influence functional is given by

$$\begin{aligned} \rho_{ss'}^{(C)}(z_f, z'_f, t) &= \int dz_i dz'_i J_{ss'}(z_f, z'_f, t; z_i, z'_i, t_0) \\ &\times \rho_{ss'}^{(C)}(z_i, z'_i, t_0), \end{aligned} \quad (5.1)$$

where the influence functional is

$$J_{ss'}(z_f, z'_f, t; z_i, z'_i, t_0) = \int \mathcal{D}z \mathcal{D}z' \exp(iS_{ss'}[z, z']), \quad (5.2)$$

$s, s' = \pm$, and the action is defined by

$$\begin{aligned} S_{ss'}[z, z'] &= S_s^0[z] - S_{s'}^0[z'] \\ &- \frac{\alpha}{2} \int_{t_0}^t d\tau [z(\tau) - z'(\tau)] [\dot{z}(\tau) + \dot{z}'(\tau)] \\ &+ \frac{i}{2} \int_{t_0}^t d\tau \int_{t_0}^t d\tau' [z(\tau) - z'(\tau)] \\ &\times K(\tau - \tau') [z(\tau') - z'(\tau')]. \end{aligned} \quad (5.3)$$

This form of the action is only valid for an Ohmic bath.²¹ Furthermore, $K(\tau)$ is the real part of the bath correlation function

$$K(\tau) \equiv \text{Re}\langle \hat{X}(\tau)\hat{X}(0) \rangle, \quad (5.4)$$

where $\hat{X}(t) = \sum_k c_k \hat{x}_k(t)$. Finally,

$$S_{ss}^0[z] = \int_{t_0}^t d\tau \left[\frac{1}{2} \dot{z}^2(\tau) - \frac{1}{2} z^2(\tau) + \eta s f(\tau) z(\tau) + \frac{1}{2} \epsilon(\tau) s \right] \quad (5.5)$$

is the bare action without oscillator bath.

The action can be simplified further by introducing relative coordinates defined by $R = (z + z')/2$ and $r = z - z'$. The action is then found to be

$$S_{ss'}[R, r] = S_{ss'}^0[R, r] - \alpha \int_{t_0}^t d\tau \dot{R}(\tau) r(\tau) + \frac{i}{2} \int_{t_0}^t d\tau \int_{t_0}^t d\tau' r(\tau) K(\tau - \tau') r(\tau'), \quad (5.6)$$

with

$$S_{ss'}^0[R, r] = \int_{t_0}^t d\tau \left\{ \dot{R}(\tau) \dot{r}(\tau) - R(\tau) r(\tau) + \eta f(\tau) R(\tau) (s - s') + \frac{1}{2} \eta f(\tau) r(\tau) (s + s') + \frac{1}{2} \epsilon(\tau) (s - s') \right\}. \quad (5.7)$$

In the next step, the action is expanded around the classical path. The classical equations of motion can be found by minimizing this action and read

$$\ddot{R}(\tau) + \alpha \dot{R}(\tau) + R(\tau) = F_R(\tau), \quad (5.8)$$

$$\ddot{r}(\tau) - \alpha \dot{r}(\tau) + r(\tau) = F_r(\tau), \quad (5.9)$$

$$F_R(\tau) = \frac{1}{2} \eta f(\tau) (s + s') + i \int_{t_0}^t d\tau' K(\tau - \tau') r(\tau'), \quad (5.10)$$

$$F_r(\tau) = \eta f(\tau) (s - s'), \quad (5.11)$$

with classical solutions $R_{cl}(\tau)$ and $r_{cl}(\tau)$, respectively. Note that the solutions are complex,²⁹ and the dependence on s, s' of all these quantities has been suppressed. The classical solutions, which are given in Appendix B, are linear in the boundary values $R_f, r_f, R_i,$ and r_i . Therefore, $S_{ss'}[R_{cl}, r_{cl}]$ is a bilinear form in these variables. We obtain

$$J_{ss'}(R_f, r_f, t; R_i, r_i, t_0) = \frac{1}{\mathcal{N}(t)} \exp(iS_{ss'}[R_{cl}, r_{cl}]), \quad (5.12)$$

where all the contributions from the fluctuations around the classical path are contained in the time-dependent, but spin-

independent, normalization constant $\mathcal{N}(t)$, which can be obtained from the normalization condition

$$\sum_{s=\pm} \int_{-\infty}^{\infty} dR_f d\rho_{ss}(R_f, r_f=0, t) = 1. \quad (5.13)$$

The Gaussian form of the expressions leads to a final reduced density matrix of Gaussian form if the initial density matrix is Gaussian, which is true for a coherent state. Therefore we deal with Gaussian wave packets also in the dissipative case. The explicit formulas are discussed in detail in Appendix B, where the solution for the reduced dynamics is obtained starting from a Gaussian wave packet at time t_0 . We then take the limit $t_0 \rightarrow -\infty$ such that the information about the initial state is lost at time $t = 0$.

We will now give analytical expressions of the density matrix for the diagonal and off-diagonal elements with respect to the spin degree of freedom. Let us first discuss the result for $s = s'$:

$$\rho_{ss}^{(C)}(R, r, t) = \frac{1}{\sqrt{2\pi\sigma_R}} \exp \left\{ -\frac{1}{2\sigma_R^2} [R - x_s(t)]^2 - \frac{1}{2\sigma_r^2} r^2 + i r \dot{x}_s(t) \right\}, \quad (5.14)$$

where the final coordinates have been replaced by $R \equiv R_f$ and $r \equiv r_f$. The widths of the Gaussian peaks are independent of the spin. The width in the R direction is given by

$$\sigma_R^2 = \int_0^\infty d\omega J_{\text{eff}}(\omega) \coth\left(\frac{\omega}{2T}\right). \quad (5.15)$$

σ_R increases with temperature. This is because the cantilever position suffers more thermal fluctuations. The width in the r direction is found to be

$$\frac{1}{\sigma_r^2} = \int_0^{\omega_C} d\omega \omega^2 J_{\text{eff}}(\omega) \coth\left(\frac{\omega}{2T}\right). \quad (5.16)$$

Note that as is well known the momentum width diverges with the cut-off frequency ω_C which was defined after Eq. (2.9). That is why we kept the dependence on the cutoff in this integral. The spin dynamics and the probability distribution of the cantilever will not depend on the cutoff. In contrast to σ_R , σ_r decreases with temperature; this is natural since the cantilever gets closer to a classical oscillator as temperature goes up. The temperature behavior of these two integrals can be read off in the limit of small $\alpha \ll 1$, viz.,

$$\sigma_R^2 \approx \frac{1}{\sigma_r^2} \approx \frac{1}{2} \coth\left(\frac{1}{2T}\right). \quad (5.17)$$

The Gaussian wave packets are moving according to

$$x_s(t) = \eta s \int_0^t dt' e^{-(\alpha/2)(t-t')} \frac{\sin[\omega_R(t-t')]}{\omega_R} f(t'), \quad (5.18)$$

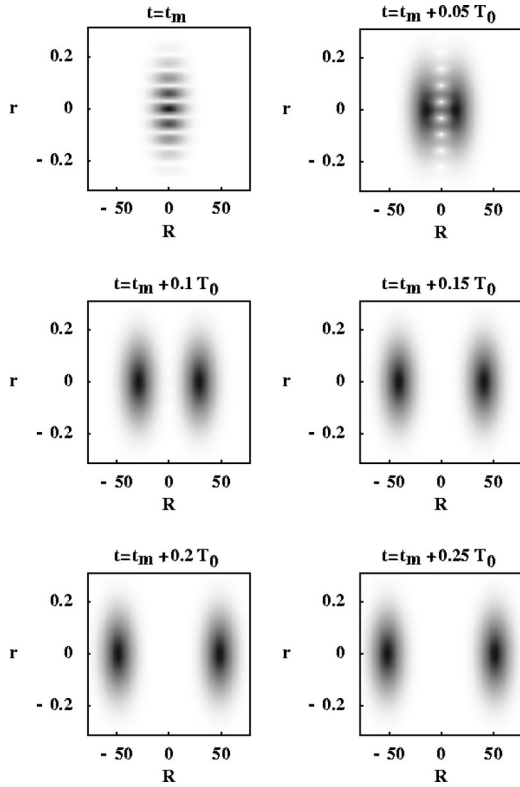


FIG. 3. $|\rho^{(C)}(R, r, t)|$ for a time series in the steady-state regime starting at time t_m at which the two peaks are not separated, e.g., $t_m=988$. The units have been chosen such that both the natural frequency ω_0 of the cantilever and its harmonic oscillator length are equal to 1. $T_0=2\pi/\omega_0$, $\alpha=0.006$, and $T=100$; the other parameters are as in the caption of Fig. 2. The interference fringes are due to the driving.

which depends on the spin s . The oscillator frequency $\omega_R = \sqrt{1 - (\alpha/2)^2}$ is renormalized due to the coupling to the bath. Furthermore, $x_s(t)$ is the solution of the coordinate of a classical dissipative driven harmonic oscillator with a spin-dependent driving force $\eta s f(t)$ starting from the initial conditions $x_s(0)=0$ and $\dot{x}_s(0)=0$. So the result becomes very clear, because the classical solution is well known to be an oscillating function, which goes through a transient regime and for $t \gg 1/\alpha$ the amplitude of the oscillation saturates at a finite value. The oscillation is periodic (but not necessarily sinusoidal) in time with unit period ($T_0=2\pi/\omega_0$). Consequently, for $t \gg 1/\alpha$ the density matrix will show a generic steady-state behavior independent of the details of the initial preparation of the system.

The density matrix $\rho_{ss}^{(C)}(R, r, t)$ behaves quite differently with respect to the coordinates R and r . As a function of R , $\rho_{ss}^{(C)}(R, r, t)$ is a Gaussian distribution with a standard deviation σ_R and average $\langle R(t) \rangle = x_s(t)$. On the other hand, $\dot{x}_s(t)$ is the velocity of a classical oscillator [see above], it shows oscillatory behavior in t and r superimposed on the Gaussian envelope with width σ_r ; see Figs. 3–6. Thus, the off-diagonal elements $\rho_{ss}^{(C)}(z, z', t)$ ($z \neq z'$) exhibit an oscillating behavior in t . However, this should not be confused with a coherent oscillation, which is not expected in this long-

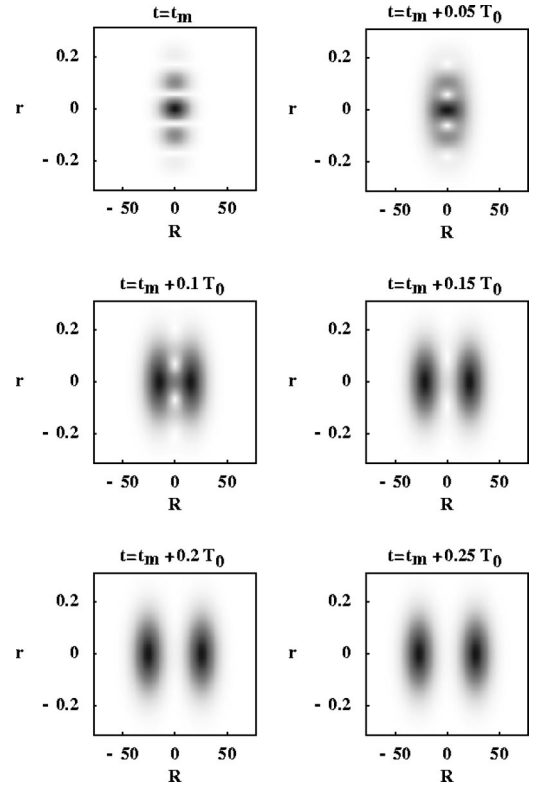


FIG. 4. $|\rho^{(C)}(R, r, t)|$ for a time series in the steady-state regime for $\alpha=0.012$ and $T=100$.

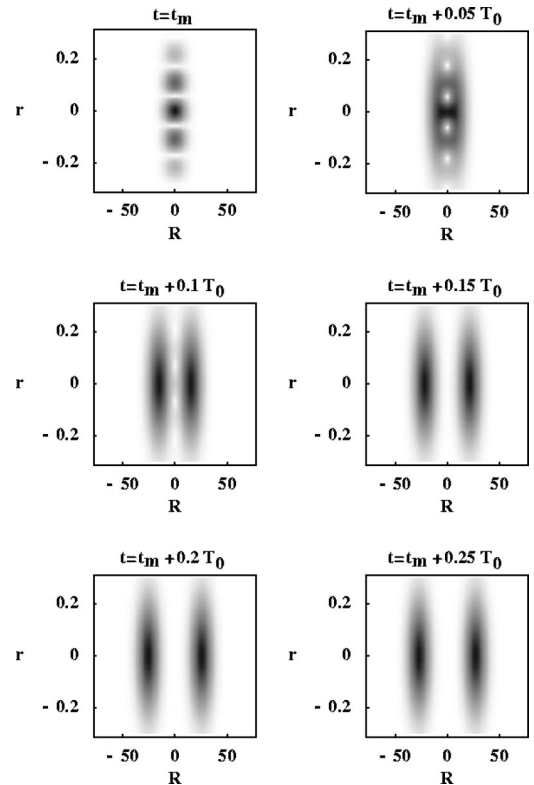


FIG. 5. $|\rho^{(C)}(R, r, t)|$ for a time series in the steady-state regime for $\alpha=0.012$ and $T=50$.

time limit. The oscillation is a consequence of the external driving $f(t)$ [i.e., frequency modulation $\dot{\phi}(t)$]. The diagonal elements (both in s and z) $\rho_{ss}^{(C)}(z, z, t)$ do not show such an oscillation.

The behavior of $x_s(t)$ can be illustrated by approximating $f(t)$ by its primary oscillation amplitude:

$$f(t) \approx f_0 \sin(t) + (\text{higher harmonics}), \quad (5.19)$$

where

$$f_0 = \frac{4}{\pi} \left(\frac{\epsilon_{\perp}}{\phi_0} \right) [E(-\phi_0^2/\epsilon_{\perp}^2) - K(-\phi_0^2/\epsilon_{\perp}^2)]. \quad (5.20)$$

Here, $K(x)$ and $E(x)$ are the complete elliptic integrals of the first and second kind.³⁰ One obtains

$$x_s(t) \approx \eta s f_0 \left(-\frac{\cos(t)}{\alpha} + e^{-(\alpha/2)t} \left[\frac{\cos(\omega_R t)}{\alpha} + \frac{\sin(\omega_R t)}{2\omega_R} \right] \right) + (\text{higher harmonics}). \quad (5.21)$$

This solution shows the main features of the spin-dependent separation $x_s(t)$, namely, the transient behavior and the steady-state oscillations: $x_s(t) \approx -\eta s f_0 \cos(t)/\alpha$. It is interesting to notice that the average cantilever motions are exactly in opposite phases (shift by π) for spin up ($s = +1$) and down ($s = -1$). This was also concluded from the numerical simulation presented Refs. 10 and 11. Thus, the MRFM can be used as a quantum measurement device, i.e., to detect the state of the spin; see below. Therefore, if we start initially with the two spin components populated, $\rho_{++}^{(S)}(0), \rho_{--}^{(S)}(0) > 0$, then $\rho^{(C)}(R, r, t) = \rho_{++}^{(S)}(0) \rho_{++}^{(C)}(R, r, t) + \rho_{--}^{(S)}(0) \rho_{--}^{(C)}(R, r, t)$ will show two peaks moving in opposite directions as time goes on; see discussions above and Figs. 3–6. It should be stressed that to separate the two peaks with sufficient resolution, the widths of the peaks, Eq. (5.15), should not be larger than the maximum separation, $\eta f_0/\alpha$; see Eq. (5.21). Clearly, this criterion restricts the maximum operation temperature of the device. Figures 3–6 show the typical behavior of the density matrix $\rho^{(C)}(R, r, t)$ of the cantilever for $\rho_{ss}^{(S)}(0) = 1/2$ for $s, s' = \pm$ as initial state. As the coupling to the environment α increases, the distance between the peaks shrinks and they are harder to distinguish; see Figs. 3 and 4. A similar behavior is observed as the temperature increases with α fixed; see Figs. 5 and 6.

Now we turn to the off-diagonal elements $s = -s'$:

$$\rho_{s,-s}^{(C)}(R, r, t) = \frac{1}{\sqrt{2\pi}\sigma_R} \exp \left\{ -\frac{1}{2\sigma_R^2} [R - i\vartheta_s(t)]^2 - \frac{1}{2\sigma_r^2} r^2 + r\zeta_s(t) - \Gamma(t) + i \int_0^t dt' \epsilon(t') \right\}, \quad (5.22)$$

where

$$\vartheta_s(t) = 2\eta s \int_0^t d\omega J_{\text{eff}}(\omega) \coth\left(\frac{\omega}{2T}\right) \times \int_0^t dt' f(t') \cos[\omega(t-t')] \quad (5.23)$$

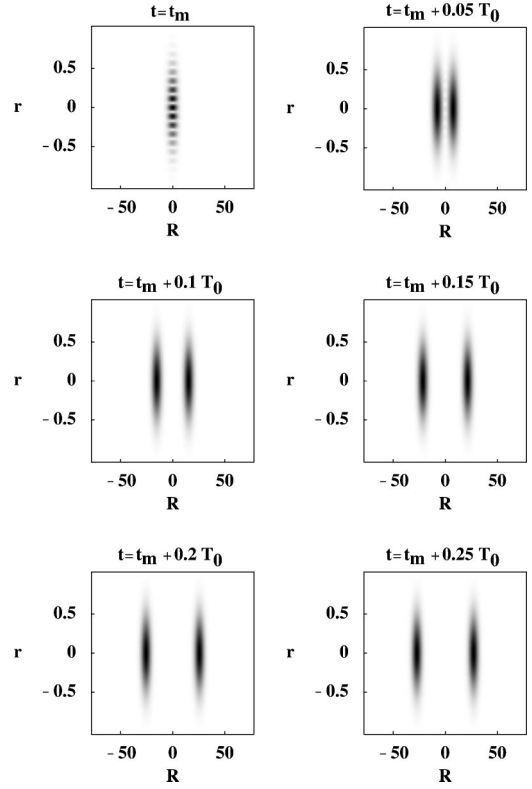


FIG. 6. $|\rho^{(C)}(R, r, t)|$ for a time series in the steady-state regime for $\alpha = 0.012$ and $T = 10$.

and

$$\zeta_s(t) = 2\eta s \int_0^\infty d\omega \omega J_{\text{eff}}(\omega) \coth\left(\frac{\omega}{2T}\right) \times \int_0^t dt' f(t') \sin[\omega(t-t')]. \quad (5.24)$$

In the r direction, $\rho_{s,-s}^{(C)}(R, r, t)$ has a Gaussian shape centered at $\zeta_s(t)/\sigma_r^2$ with width σ_r . In the R direction, it is an oscillatory function imposed on a Gaussian envelope with width σ_R . Overall, the function $\rho_{s,-s}^{(C)}(R, r, t)$ decays with t in the same way as shown in Fig. 2, i.e., $\rho_{ss'}^{(C)}(R, r, t)$ for $s \neq s'$ can be observed only in the transient regime. The decay is described by the function $\Gamma(t)$; see Eq. (4.11). Note that a trace over the cantilever dynamics leads us back to the results obtained in a much simpler way in Sec. IV.

VI. MRFM AS A QUANTUM MEASUREMENT DEVICE

One of the conclusions of the analysis presented here is that the cantilever oscillates with the same amplitude for both initial spin states (up and down). Probing the amplitude of the cantilever vibration can only tell the absolute value of the spin in the direction of $\mathbf{B}_{\text{eff}}(0)$, but not its sign. However, the oscillations for the initial spin up and down states are completely out of phase (phase difference of π); see Sec. V. This fact was also noticed by Berman *et al.*¹⁰ in their numerical simulations. Hence, there is the possibility to use the MRFM as a quantum measurement device, i.e., to detect the direction of the spin with the MRFM by probing the (dis-

crete) relative phases of the cantilever oscillations. In the quantum theory of measurement, this falls into the category of the indirect quantum measurement scheme.¹⁴ In such a scheme, the quantum object supposed to be measured is coupled to another quantum system, the so-called quantum probe. The classical measurement device then detects the quantum probe instead of probing directly the quantum object. In our case, the quantum object is the spin, the quantum probe corresponds to the cantilever, and the classical measurement device can be, e.g., the fiber-optical interferometer. A conceivable scheme to measure the relative phases of the cantilever oscillations is to use a reference spin which is prepared in a definite known state, for example, by applying a strong magnetic field in a desired direction. The two signals from the reference spin and the spin in an unknown state are superposed to determine the relative phase of the unknown spin.

VII. CONCLUSIONS

We have studied the CAI-based MRFM as a high-resolution tool to detect single spins. The quantum dynamics of the spin-plus-cantilever system was analyzed in terms of the reduced density matrices, $\hat{\rho}^{(S)}(t)$ (for the spin) and $\hat{\rho}^{(C)}(t)$ (for the cantilever), in the presence of coupling to the environment. Using an effective bath model, we were able to determine the dynamics of the spin during the measurement process. Our results remain valid at all temperatures as long as the adiabatic approximation is satisfied. We have evaluated the influence functional for the combined system of spin and cantilever to obtain the quantum dissipative dynamics of the cantilever. These results are valid for all temperatures and coupling strengths. Finally, we have proposed that the MRFM can be used as a quantum measurement device, i.e., not only to detect the absolute value of the spin but also to detect its direction.

The dissipative dynamics of an open quantum system is sensitive to the low-frequency behavior of the spectral density of the environment. While the Ohmic model Eq. (2.9) is a plausible model, it will be worthwhile to identify the sources of the environmental fluctuations and construct a physical model of the environment starting from a more microscopic theory of the cantilever.

ACKNOWLEDGMENTS

We would like to thank V. Cerletti, F. Meier, and particularly F. Marquardt for helpful discussions. Our work was supported by the SKORE-A program, the Swiss NSF, the NCCR Nanoscience, and the eSSC at Postech. H.G. and M.-S.C. acknowledge the support by KIAS, where part of the work was done. M.-S.C. was supported by a Korea Research Foundation Grant (KRF-2002-070-C00029).

APPENDIX A: ESTIMATION OF THE SPIN-FLIP RATE

The cyclic adiabatic inversion scheme implies two basic assumptions: (i) The variation of the external driving $\dot{\phi}(t)$ is slow enough to allow for an adiabatic approximation,¹⁸ i.e.,

$|\ddot{\phi}(t)| \ll \epsilon_{\perp}^2$. (ii) The time scales of the spin dynamics and the cantilever dynamics are well separated ($\epsilon_{\perp} \gg 1$) such that the Born-Oppenheimer approximation is justified. Yet, the finite rates of change in the external driving and the cantilever position will induce spin-flips. The spin-flip rate can be estimated by the Landau-Zener transition (adiabatic transition) rate.^{19,31-34} For this purpose, we rewrite Eqs. (2.4) and (2.8) in the form

$$\mathcal{H}_{LZ}(t) = -\frac{1}{2}F(t)\hat{\sigma}_z - \frac{1}{2}\epsilon_{\perp}\hat{\sigma}_x, \quad (\text{A1})$$

where $F(t) \equiv \dot{\phi}(t) + 2\eta\langle\dot{z}(t)\rangle$. The back-action of the cantilever has been accounted for by its time-dependent average position, and the contribution from it will be estimated below in a self-consistent way based on the results in Sec. V. The probability that the spin-flips against the effective magnetic field $\mathbf{B}_{\text{eff}}(t)$ during one period (i.e., $2\pi/\omega_0$) is then given by

$$P_{LZ} \approx \exp\left(-\frac{\pi\epsilon_{\perp}^2}{\nu}\right), \quad (\text{A2})$$

where we have taken $\nu \equiv \max|\dot{F}(t)|$ to estimate the worst case.

It follows from Eqs. (2.5) and (5.21) that

$$\nu \leq \max|\ddot{\phi}(t)| + 2\eta \max\left|\frac{d}{dt}\langle\dot{z}(t)\rangle\right| = \phi_0 + 2\frac{\eta^2}{\alpha}f_0. \quad (\text{A3})$$

Therefore, assuming typical values for the parameters, $\phi_0 \sim 1000$, $\epsilon_{\perp} \sim 400$, $\eta \sim 1$, and $\alpha \sim 0.001$, we have $f_0 \sim 1$ and

$$P_{LZ} < \exp\left(-\pi\frac{\epsilon_{\perp}^2}{\phi_0 + 2\eta^2f_0/\alpha}\right) \sim 10^{-70}. \quad (\text{A4})$$

Note that the back-action of the cantilever is stronger for larger Q factors of the cantilever ($Q \approx 1/\alpha$) since the maximum velocity of the cantilever increases with the Q factor.

APPENDIX B: PATH-INTEGRAL FORMULAS

In this appendix we will fill in some of the details left out in Sec. V. It is convenient to define $\gamma \equiv \alpha/2$ as the friction constant.

The classical solutions to Eqs. (5.8) and (5.9) are given by

$$r_{cl}(\tau) = \frac{1}{\sin[\omega_R(t-t_0)]} \{r_i \sin[\omega_R(t-\tau)]e^{\gamma(\tau-t_0)} + [r_f - r_p(t)] \sin[\omega_R(\tau-t_0)]e^{\gamma(\tau-t)}\} + r_p(\tau), \quad (\text{B1})$$

$$R_{cl}(\tau) = \frac{1}{\sin[\omega_R(t-t_0)]} \{R_i \sin[\omega_R(t-\tau)]e^{-\gamma(\tau-t_0)} + [R_f - R_p(t)] \sin[\omega_R(\tau-t_0)]e^{-\gamma(\tau-t)}\} + R_p(\tau), \quad (\text{B2})$$

where

$$r_p(\tau) = \int_{t_0}^{\tau} d\tau' G_r(\tau - \tau') F_r(\tau'), \quad (\text{B3})$$

$$R_p(\tau) = \int_{t_0}^{\tau} d\tau' G_R(\tau - \tau') F_R(\tau'), \quad (\text{B4})$$

and the Green's functions are defined by

$$G_R(\tau) = \Theta(\tau) e^{-\gamma\tau} \frac{\sin(\omega_R \tau)}{\omega_R}, \quad (\text{B5})$$

$$G_r(\tau) = \Theta(\tau) e^{\gamma\tau} \frac{\sin(\omega_R \tau)}{\omega_R}. \quad (\text{B6})$$

The influence functional for $s' = s$ is found to be

$$\begin{aligned} J_{ss}(R_f, r_f, t; R_i, r_i, t_0) &= \frac{|N(t)|}{2\pi} \exp\{i[K_f(t)R_f r_f + K_i(t)R_i r_i - L(t)R_i r_f \\ &\quad - N(t)R_f r_i + a_i(t)r_i + a_f(t)r_f] - A(t)r_f^2 \\ &\quad - B(t)r_f r_i - C(t)r_i^2\}, \end{aligned} \quad (\text{B7})$$

where the functions appearing in the influence functional are all real and defined by

$$K_f(t) = \omega_R \cot[\omega_R(t - t_0)] - \gamma, \quad (\text{B8})$$

$$K_i(t) = \omega_R \cot[\omega_R(t - t_0)] + \gamma, \quad (\text{B9})$$

$$L(t) = \frac{\omega_R e^{-\gamma(t-t_0)}}{\sin[\omega_R(t-t_0)]}, \quad (\text{B10})$$

$$N(t) = \frac{\omega_R e^{\gamma(t-t_0)}}{\sin[\omega_R(t-t_0)]}, \quad (\text{B11})$$

$$\begin{aligned} A(t) &= \frac{1}{2} \frac{e^{-2\gamma t}}{\sin^2[\omega_R(t-t_0)]} \int_{t_0}^t d\tau \int_{t_0}^{\tau} d\tau' \sin[\omega_R(\tau - t_0)] \\ &\quad \times K(\tau - \tau') \sin[\omega_R(\tau' - t_0)] e^{\gamma(\tau + \tau')}, \end{aligned} \quad (\text{B12})$$

$$\begin{aligned} B(t) &= \frac{e^{-\gamma(t+t_0)}}{\sin^2[\omega_R(t-t_0)]} \int_{t_0}^t d\tau \int_{t_0}^{\tau} d\tau' \sin[\omega_R(t-\tau)] \\ &\quad \times K(\tau - \tau') \sin[\omega_R(\tau' - t_0)] e^{\gamma(\tau + \tau')}, \end{aligned} \quad (\text{B13})$$

$$\begin{aligned} C(t) &= \frac{1}{2} \frac{e^{-2\gamma t_0}}{\sin^2[\omega_R(t-t_0)]} \int_{t_0}^t d\tau \int_{t_0}^{\tau} d\tau' \sin[\omega_R(t-\tau)] \\ &\quad \times K(\tau - \tau') \sin[\omega_R(t-\tau')] e^{\gamma(\tau + \tau')}, \end{aligned} \quad (\text{B14})$$

$$a_f(t) = \dot{x}(t) - K_f(t)x(t), \quad (\text{B15})$$

$$a_i(t) = N(t)x(t), \quad (\text{B16})$$

$$x(\tau) = \eta s \int_{t_0}^{\tau} d\tau' G_R(\tau - \tau') f(\tau'), \quad (\text{B17})$$

$$\dot{x}(\tau) = \eta s \int_{t_0}^{\tau} d\tau' \partial_{\tau} G_R(\tau - \tau') f(\tau'). \quad (\text{B18})$$

In all of these expressions, the dependence on t_0 has been suppressed.

Let us now discuss the solution for the density matrix. At time $t = t_0$ we start in a product state between the cantilever and bath. The cantilever density matrix is assumed to be a Gaussian wave packet with a width σ at $t = t_0$,

$$\rho_{ss'}^{(C)}(z, z', t_0) = \frac{1}{\sqrt{2\pi}\sigma} \exp\left(-\frac{1}{4\sigma^2}(z^2 + z'^2)\right). \quad (\text{B19})$$

One could start from a more general initial state, but we will later take the limit $t_0 \rightarrow -\infty$, such that all the information on the initial state is lost completely at time $t = 0$. The experiment starts at time $t = 0$ by switching on the magnetic field. At this time the cantilever has interacted with the bath for a very long time and is in equilibrium with the bath, i.e., not any more in a product state.

The general solution for the diagonal elements of $\rho_{ss'}^{(C)}$ starting from this initial condition is

$$\begin{aligned} \rho_{ss}^{(C)}(R_f, r_f, t) &= \frac{|N(t)|}{\sqrt{2\pi}} \frac{2\sigma}{\sqrt{D(t)}} \exp\left\{\left[r_f^2 \left(-A(t) + \left[2B^2(t) - 8A(t)C(t) - \frac{L^2(t)}{2}\right] \sigma^2 \right. \right. \right. \\ &\quad \left. \left. - 4\{A(t)K_i^2(t) + L(t)[B(t)K_i(t) + C(t)L(t)]\} \sigma^4\right) + ir_f \{a_f(t) - 4[a_i(t)B(t) - 2a_f(t)C(t)] \sigma^2 \right. \\ &\quad \left. + 4K_i(t)[a_f(t)K_i(t) + a_i(t)L(t)] \sigma^4\} + iR_f r_f \{K_f(t) + 4[2C(t)K_f(t) + B(t)N(t)] \sigma^2 \right. \\ &\quad \left. + 4K_i(t)[K_f(t)K_i(t) - L(t)N(t)] \sigma^4\} - 2[a_i(t) - N(t)R_f]^2 \sigma^2 \right\} / D(t), \end{aligned} \quad (\text{B20})$$

where

$$D(t) = 1 + 8C(t)\sigma^2 + 4K_i^2(t)\sigma^4. \quad (\text{B21})$$

In the limit $t_0 \rightarrow -\infty$ we obtain the final result presented in Eq. (5.14).

The influence functional for $s' = -s$ is found to be given by

$$J_{s,-s}(R_f, r_f, t; R_i, r_i, t_0) = \frac{|N(t)|}{2\pi} \exp\left(i \left[K_f(t) R_f r_f + K_i(t) R_i r_i - L(t) R_i r_f - N(t) R_f r_i + A_f(t) R_f + A_i(t) R_i + \int_{t_0}^t d\tau \epsilon(\tau) \right] \right) \\ \times \exp[-A(t)r_f^2 - B(t)r_f r_i - C(t)r_i^2 + b_i(t)r_i + b_f(t)r_f + b(t)], \quad (\text{B22})$$

where

$$A_f(t) = \dot{y}(t) - K_i(t)y(t), \quad (\text{B23})$$

$$A_i(t) = L(t)y(t), \quad (\text{B24})$$

$$b_f(t) = 2A(t)y(t) - \int_{t_0}^t d\tau \int_{t_0}^t d\tau' y(\tau') \\ \times K(\tau - \tau') \frac{\sin[\omega_R(\tau - t_0)] e^{-\gamma(t-\tau)}}{\sin[\omega_R(t - t_0)]}, \quad (\text{B25})$$

$$b_i(t) = B(t)y(t) - \int_{t_0}^t d\tau \int_{t_0}^t d\tau' y(\tau') \\ \times K(\tau - \tau') \frac{\sin[\omega_R(t - \tau)] e^{\gamma(\tau-t_0)}}{\sin[\omega_R(t - t_0)]}, \quad (\text{B26})$$

$$b(t) = -A(t)y^2(t) + y(t) \int_{t_0}^t d\tau \int_{t_0}^t d\tau' y(\tau') \\ \times K(\tau - \tau') \frac{\sin[\omega_R(\tau - t_0)] e^{-\gamma(t-\tau)}}{\sin[\omega_R(t - t_0)]} \\ - \frac{1}{2} \int_{t_0}^t d\tau \int_{t_0}^t d\tau' y(\tau) K(\tau - \tau') y(\tau'), \quad (\text{B27})$$

$$y(\tau) = 2\eta s \int_{t_0}^{\tau} d\tau' G_r(\tau - \tau') f(\tau'), \quad (\text{B28})$$

$$\dot{y}(\tau) = 2\eta s \int_{t_0}^{\tau} d\tau' \partial_{\tau} G_r(\tau - \tau') f(\tau'). \quad (\text{B29})$$

This leads to the following general expression for the off-diagonal elements of $\rho_{ss'}^{(C)}$:

$$\rho_{s,-s}^{(C)}(R_f, r_f, t) = \frac{|N(t)|}{\sqrt{2\pi}} \frac{2\sigma}{\sqrt{D(t)}} \exp\left\{ \left[r_f^2 \left(-A(t) + \left[2B^2(t) - 8A(t)C(t) - \frac{L^2(t)}{2} \right] \sigma^2 - 4\{A(t)K_i^2(t) + L(t)[B(t)K_i(t) \right. \right. \right. \\ \left. \left. \left. + C(t)L(t)\} \right] \sigma^4 + r_f \{ b_f(t) + [-4B(t)b_i(t) + 8b_f(t)C(t) + A_i(t)L(t)] \sigma^2 + 4[A_i(t)B(t)K_i(t) \right. \right. \\ \left. \left. + b_f(t)K_i^2(t) + 2A_i(t)C(t)L(t) + b_i(t)K_i(t)L(t) \right] \sigma^4 + iR_f r_f \{ K_f(t) + 4[2C(t)K_f(t) + B(t)N(t)] \sigma^2 \right. \\ \left. \left. + 4K_i(t)[K_f(t)K_i(t) - L(t)N(t)] \sigma^4 + iR_f \{ A_f(t) + 8A_f(t)C(t) \sigma^2 + 4K_i(t)[A_f(t)K_i(t) + A_i(t)N(t)] \sigma^4 \right. \right. \\ \left. \left. + 2[b_i(t) - iN(t)R_f]^2 \sigma^2 - \frac{A_i^2(t)}{2} \sigma^2 - 4A_i(t)[A_i(t)C(t) + b_i(t)K_i(t)] \sigma^4 \right] \right\} / \left[D(t) + i \int_{t_0}^t d\tau \epsilon(\tau) + b(t) \right]. \quad (\text{B30})$$

The reduced dynamics of the spin alone is found by tracing out the cantilever coordinates. The result is

$$\rho_{s,-s}^{(S)}(t) = \rho_{s,-s}^{(S)}(0) \exp\left(-A_f^2(t) \frac{C(t)}{N^2(t)} + \frac{A_f(t)b_i(t)}{N(t)} + b(t) - \frac{A_f^2(t)}{8\sigma^2 N^2(t)} - \frac{\sigma^2}{2N^2(t)} [A_f(t)K_i(t) + A_i(t)N(t)]^2 + i \int_{t_0}^t d\tau \epsilon(\tau) \right) \\ \equiv \rho_{s,-s}^{(S)}(0) \exp\left(-\Gamma(t) + i \int_{t_0}^t d\tau \epsilon(\tau) \right). \quad (\text{B31})$$

The decay rate $\Gamma(t)$ [see Eq. (4.11)], can be obtained in the limit $t_0 \rightarrow -\infty$ after a straightforward but tedious calculation. In the same limit, we get the result for the density matrix presented in Eq. (5.22).

- *Electronic address: hanno.gassmann@unibas.ch
 †Electronic address: choims@korea.ac.kr
- ¹C.P. Slichter, *Principles of Magnetic Resonance*, 3rd ed. (Springer-Verlag, Berlin, 1990).
 - ²J.A. Sidles, J.L. Garbini, K.J. Bruland, D. Rugar, O. Züger, S. Hoen, and C.S. Yannoni, *Rev. Mod. Phys.* **67**, 249 (1995).
 - ³M.F. Bocko and R. Onofrio, *Rev. Mod. Phys.* **68**, 755 (1996).
 - ⁴H.J. Mamin and D. Rugar, *Appl. Phys. Lett.* **79**, 3358 (2001).
 - ⁵T.D. Stowe, K. Yasumura, T.W. Kenny, D. Botkin, K. Wago, and D. Rugar, *Appl. Phys. Lett.* **71**, 288 (1997).
 - ⁶X.M.H. Huang, C.A. Zorman, M. Mehregany, and M.L. Roukes, *Nature (London)* **421**, 496 (2003).
 - ⁷A. Abramovici *et al.*, *Phys. Lett. A* **218**, 157 (1996).
 - ⁸R.G. Knobel and A.N. Cleland, *Nature (London)* **424**, 291 (2003).
 - ⁹D. Mozyrsky, I. Martin, D. Pelekhov, and P.C. Hammel, *Appl. Phys. Lett.* **82**, 1278 (2003).
 - ¹⁰G.P. Berman, F. Borgonovi, G. Chapline, S.A. Gurvitz, P.C. Hammel, D.V. Pelekhov, A. Suter, and V.I. Tsifrinovich, *J. Phys. A* **36**, 4417 (2003).
 - ¹¹G.P. Berman, F. Borgonovi, H.S. Goan, S.A. Gurvitz, and V.I. Tsifrinovich, *Phys. Rev. B* **67**, 094425 (2003).
 - ¹²G. Lindblad, *Commun. Math. Phys.* **48**, 119 (1976).
 - ¹³L. Diósi, *Physica A* **199**, 517 (1993).
 - ¹⁴H.-P. Breuer and F. Petruccione, *The Theory of Open Quantum Systems* (Oxford University Press, New York, 2002).
 - ¹⁵U. Weiss, *Quantum Dissipative Systems*, 2nd ed. (World Scientific, Singapore, 2000).
 - ¹⁶R. Feynman and F. Vernon, *Ann. Phys. (N.Y.)* **24**, 118 (1963).
 - ¹⁷H. Grabert, P. Schramm, and G.-L. Ingold, *Phys. Rep.* **168**, 115 (1988).
 - ¹⁸A. Messiah, *Quantum Mechanics* (North-Holland, Amsterdam, 1961), Vol. II.
 - ¹⁹J.E. Avron, R. Seiler, and L.G. Yaffe, *Commun. Math. Phys.* **110**, 33 (1987).
 - ²⁰N.W. Ashcroft and N.D. Mermin, *Solid State Physics* (Holt Rinehart and Winston, New York, 1976).
 - ²¹A.O. Caldeira and A.J. Leggett, *Physica A* **121**, 587 (1983).
 - ²²A.O. Caldeira and A.J. Leggett, *Ann. Phys. (N.Y.)* **149**, 374 (1983).
 - ²³A.O. Caldeira and A.J. Leggett, *Phys. Rev. Lett.* **46**, 211 (1981).
 - ²⁴C.W. Gardiner and P. Zoller, *Quantum Noise*, 2nd ed. (Springer-Verlag, Berlin, 2000).
 - ²⁵A. Garg, J.N. Onuchic, and V. Ambegaokar, *J. Chem. Phys.* **83**, 4491 (1985).
 - ²⁶H. Gassmann, F. Marquardt, and C. Bruder, *Phys. Rev. E* **66**, 041111 (2002).
 - ²⁷F.K. Wilhelm, *Phys. Rev. B* **68**, 060503 (2003).
 - ²⁸S. Kleff, S. Kehrein, and J. von Delft, cond-mat/0302357 (unpublished).
 - ²⁹F. Marquardt, cond-mat/0207692 (unpublished).
 - ³⁰*Handbook of Mathematical Functions with Formulas, Graphs, and Mathematical Tables*, edited by M. Abramowitz and I.A. Stegun (Wiley, New York, 1972).
 - ³¹M. Grifoni and P. Hänggi, *Phys. Rep.* **304**, 229 (1998).
 - ³²L.D. Landau, *Phys. Z. Sowjetunion* **1**, 89 (1932).
 - ³³C. Zener, *Proc. Phys. Soc. London* **137**, 696 (1932).
 - ³⁴E.G.C. Stückelberg, *Helv. Phys. Acta* **5**, 369 (1932).